

Three-State Anti-ferromagnetic Potts Model in Three Dimensions: Universality and Critical Amplitudes

Aloysius P. Gottlob

Universität Kaiserslautern, D-67653 Kaiserslautern, Germany

and

Martin Hasenbusch

CERN, Theory Division, CH-1211 Genève 23, Switzerland

Abstract

We present the results of a Monte Carlo study of the three-dimensional anti-ferromagnetic 3-state Potts model. We compute various cumulants in the neighbourhood of the critical coupling. The comparison of the results with a recent high statistics study of the 3D XY model strongly supports the hypothesis that both models belong to the same universality class. From our numerical data of the anti-ferromagnetic 3-state Potts model we obtain for the critical coupling $K_c = 0.81563(3)$, and for the static critical exponents $\gamma/\nu = 1.973(9)$ and $\nu = 0.664(4)$.

I. INTRODUCTION

Restoration of symmetries plays a crucial role in lattice field theory. The Euclidean invariance is broken by the lattice. In order to recover the continuum field theory, the Euclidean symmetry has to be restored in the critical limit of the lattice theory [1].

Symmetries of the spin-manifold might also be enhanced: the Hamiltonian of the discrete Gaussian model has only \mathbb{Z} symmetry, while for sufficiently high temperature the renormalization group fixed point of the 2D system is Gaussian, possessing \mathbb{R} invariance [2].

In a similar fashion the 3D anti-ferromagnetic (AF) 3-state Potts model is believed to restore $U(1)$ symmetry at the critical point. Banavar, Grest and Jasnow [3] conjectured, based on ϵ -expansion and Monte Carlo simulations, that the AF 3-state Potts model in three dimensions undergoes a second-order phase transition and that it shares the universality class with the $O(2)$ vector model. They expect an analogous result for the AF 4-state Potts model, sharing universality with the $O(3)$ vector model. Hoppe and Hirst [4] concluded from their Monte Carlo simulation that the AF 5-state Potts model still has a second-order phase transition, while the AF 6-state Potts model does not undergo a phase transition at all.

A different point of view is taken by Ono [5], who claims to find a Kosterlitz-Thouless phase transition for the 3D AF 3-state Potts model. Ueno et al. [6] read from their Monte Carlo data that the 3D AF 3-state Potts model exhibits a second-order phase transition but with critical exponents different from the $O(N)$ -invariant universality.

Wang et al. [7] later simulated the 3D AF 3-state Potts model using the cluster algorithm and found critical exponents in reasonable agreement with those of the 3D XY model obtained by field theoretical methods [8–10].

In order to clarify this issue we simulated the 3D AF 3-state Potts model using the single cluster algorithm proposed by Wang et al. [7], with high statistics.

Privman et al. [11] pointed out that, in addition to critical exponents, universality classes are characterized by critical amplitudes. In a numerical study, their values can be obtained more accurately than those of critical exponents; hence we determined carefully various cumulants at the critical point [12]. It turned out to be crucial to use an appropriate order parameter, that allows us to detect the restoration of the $U(1)$ -symmetry at criticality.

This paper is organized as follows. In section 2 we discuss various choices of order parameters and give definitions of quantities we are measuring. In section 3 we discuss our numerical results. We give a comparison of our results with previous studies of the 3D AF 3-state Potts model and 3D XY model in section 4. Finally section 5 contains our conclusions.

II. ORDER PARAMETER AND CUMULANTS

The 3-state Potts model in three dimensions is defined by the partition function

$$\mathcal{Z} = \prod_{l \in \Lambda} \sum_{\sigma_l=1}^3 \exp(K \sum_{\langle i,j \rangle} \delta_{\sigma_i, \sigma_j}), \quad (2.1)$$

where the summation is taken over all nearest neighbour pairs of sites i and j on a simple cubic lattice Λ and $K = \frac{J}{k_b T}$ is the reduced inverse temperature. The 3-state Potts model can be transformed into the \mathbb{Z}_3 clock model

$$\mathcal{Z} = \mathcal{Z}_0 \prod_{l \in \Lambda} \sum_{\vec{s}_l \in \mathbb{Z}_3} \exp(\widetilde{K} \sum_{\langle i,j \rangle} \vec{s}_i \cdot \vec{s}_j), \quad (2.2)$$

where $\mathcal{Z}_0 = \exp(-\frac{1}{3}KDV)$ with V being the volume of the lattice and $\widetilde{K} = \frac{2}{3}K$. In the following we will consider anti-ferromagnetic interactions $J < 0$.

For the definition of an order parameter we map the anti-ferromagnetic model onto a ferromagnetic one. Therefore we subdivide the simple cubic lattice into two sub-lattices Λ^a and Λ^b in checker-board fashion, and obtain a positive sign of the coupling by redefining the spins on one of the sub-lattices

$$\begin{aligned} \vec{s}_i' &= \vec{s}_i & \text{for } i \in \Lambda^a, \\ \vec{s}_i' &= -\vec{s}_i & \text{for } i \in \Lambda^b. \end{aligned} \quad (2.3)$$

Hence we obtain for the magnetization of the ferromagnetic redefined model

$$\begin{aligned} \vec{M} &= \sum_{i \in \Lambda} \vec{s}_i' \\ &= \sum_{i \in \Lambda^a} \vec{s}_i - \sum_{i \in \Lambda^b} \vec{s}_i. \end{aligned} \quad (2.4)$$

Note that this definition of the magnetization is the same as the one given by Ono [5]. Wang et al. [7] used a variant choice of the order parameter. They define

$$m_\mu = \frac{2}{L^D} \left(\sum_{i \in \Lambda^a} \delta_{\sigma_i, \mu} - \sum_{i \in \Lambda^b} \delta_{\sigma_i, \mu} \right), \quad (2.5)$$

where μ takes the values 1, 2, 3 and the order parameter is given by

$$\widetilde{M} = \frac{1}{3} \sum_{\mu=1}^3 |m_\mu|. \quad (2.6)$$

It is not obvious how the restoration of the $U(1)$ symmetry can be detected using this order parameter, hence in the following we only consider \vec{M} .

The energy density E of the model is given by

$$E = \frac{1}{3L^3} \sum_{\langle i,j \rangle} \langle \delta_{\sigma_i, \sigma_j} \rangle. \quad (2.7)$$

The magnetic susceptibility χ gives the reaction of the magnetization to an external field. In the high temperature phase one gets

$$\chi = \frac{1}{L^3} \langle \vec{M}^2 \rangle, \quad (2.8)$$

since $\langle \vec{M} \rangle = 0$. At the critical point the susceptibility diverges as

$$\chi \sim L^{\frac{\gamma}{\nu}}, \quad (2.9)$$

where ν is the critical exponent of the correlation length and γ the critical exponent of the susceptibility.

We studied the fourth-order cumulant of the magnetization

$$U_L = 1 - \frac{1}{3} \frac{\langle \vec{M}^4 \rangle}{\langle \vec{M}^2 \rangle^2}. \quad (2.10)$$

In addition we consider the magnetization on sub-blocks of size $L/2$. We computed the fourth order cumulants defined on these sub-blocks and a normalized nearest-neighbour product

$$NN = \frac{\langle \vec{M}_I \vec{M}_J \rangle}{\langle \vec{M}_I^2 \rangle}, \quad (2.11)$$

where I and J are nearest-neighbour-blocks. At the critical point the cumulants should converge to a universal fixed point. This property is used to determine the critical coupling [13].

III. NUMERICAL RESULTS

In the present work we employ the single cluster algorithm proposed by Wang et al. [7]. In the ferromagnetic \mathbb{Z}_3 parametrization of eq.(2.3) this algorithm can be understood as the single cluster algorithm introduced by Wolff [14], with the reflection planes restricted by the \mathbb{Z}_3 symmetry.

On lattices of the size $L = 4, 8, 16, 32$ and 64 we have performed simulations at $K_0 = 0.8157$, which is the estimate for the critical coupling obtained in ref. [7]. We performed N measurements taken every N_0 update steps. We have chosen N_0 such that on average the lattice is updated approximately twice for one measurement. The results of the runs are summarized in Table I.

A. Critical coupling

First we determined the critical coupling K_c , employing Binder's phenomenological renormalization group method [13].

For the extrapolation of the observables, entering the cumulants, to couplings K other than the simulation coupling K_0 , we used the reweighting formula [15]

$$\langle A \rangle(K) = \frac{\sum_i A_i \exp((-K + K_0)H_i)}{\sum_i \exp((-K + K_0)H_i)}, \quad (3.1)$$

where i labels the configurations generated according to the Boltzmann-weight at K_0 . We computed the statistical errors from Jackknife binning [16] on the final result of the extrapolated cumulants. The extrapolation gives good results only within a small neighbourhood of the simulation coupling K_0 . This range shrinks with increasing volume of the lattice. However, the figs. 1 a)-c) show that the extrapolation performs well in a sufficiently large neighbourhood of the crossings of the cumulants.

When one considers the cumulants as functions of the coupling, the crossings of the curves for different L provide an estimate for the critical coupling K_c . The results for the crossings are summarized in Table II.

The convergence of the crossings of NN towards K_c seems to be slower than that of the fourth-order cumulants, but it is interesting to note that the K_{cross} for the fourth-order cumulant and NN come from different sides with increasing L . This is shown in fig. 2, where the estimates of K_{cross} versus the lattice size L are plotted. This behaviour we also observed for the 3D XY model [17]. The given errors are calculated with a jackknife procedure. The convergence of the crossing coupling K_{cross} towards K_c should follow

$$K_{cross}(L) = K_c (1 + const.L^{-(\omega+\frac{1}{\nu})} + \dots), \quad (3.2)$$

where ω is the correction to scaling exponent [18,13]. We performed a two-parameter fit for the crossings of the cumulants, keeping the exponents fixed to $\omega = 0.780$ and $\nu = 0.669$ [10], following the above formula. It is important to note that the value of K_c does not depend strongly on the value of the exponents. Our final estimate for the critical coupling is $K_c = 0.81563(3)$, obtained from the two-parameter fit eq.(3.2) of the fourth-order cumulants. For the cumulant on the sub-block we have to discard the 4 – 8 crossing to obtain a fit with an acceptable χ^2/dof . The results of the fits are summarized in Table III.

B. Critical amplitudes

At the critical coupling K_c the cumulants converge with increasing lattice size L to an universal fixed point. The results of the cumulants at $K = 0.81560, 0.81563$ and 0.81566 , which are our best estimate of the critical coupling and the edges of the error-bar, are given in Table IV.

The convergence rate is given by [13]

$$U_L(K_c) = U_\infty (1 + const.L^{-\omega} + \dots). \quad (3.3)$$

We performed a two-parameter fit with $\omega = 0.780$ [10] being fixed. The results of the fits are given in Table V. We had to discard the data from $L = 4$ in order to obtain an acceptable χ^2/dof . The results of the fits are stable when discarding the $L = 8$ data point.

As our final estimates we obtain

Final estimates

Model	K_c	U_L	$U_{L/2}$	NN
Potts	0.81563(3)	0.5861(6)	0.5465(6)	0.8123(9)
XY	0.45419(2)	0.5875(28)	0.5477(25)	0.8144(37)

where we have taken into account the uncertainty of the critical coupling K_c . For comparison we give the analogous results for the 3D XY model.

A careful reanalysis, taking into account eq.(3.2), leads to a small shift in K_c compared to ref. [17] where we quoted $K_c = 0.45420(2)$ as final result. This shift of the coupling also implies a slight change in the result for the cumulants. The higher accuracy of the values for the Potts model is due to higher statistics and to a smaller variation of the fit results within the error-bars of the critical coupling.

Note that the accurately determined values of the cumulants of the two models coincide within the error-bars. This fact strongly favours the hypothesis that the two models belong to the same universality class.

C. Critical exponents

We extracted the critical exponent ν of the correlation length from the L dependence of the slope of the fourth-order cumulants and the nearest-neighbour observable at the estimated critical coupling [13]. According to Binder, the scaling relation for the slope of the fourth-order cumulant is given by

$$\left. \frac{\partial U(L, K)}{\partial K} \right|_{K_c} \propto L^{1/\nu}. \quad (3.4)$$

We evaluated the slopes of the observables A entering the cumulant U according to

$$\frac{\partial \langle A \rangle}{\partial K} = \langle AH \rangle - \langle A \rangle \langle H \rangle, \quad (3.5)$$

where A is an observable and H is the energy. The statistical errors are calculated from a Jackknife analysis for the value of the slope. First we estimated the exponent ν from different lattices via

$$\nu = \frac{\ln(L_2) - \ln(L_1)}{\ln \left(\left. \frac{\partial A(L_2, K)}{\partial K} \right|_{K_c} \right) - \ln \left(\left. \frac{\partial A(L_1, K)}{\partial K} \right|_{K_c} \right)}. \quad (3.6)$$

The results are given in Table VI. Since the statistical errors are small one can check the convergence of ν obtained from the pair of lattice sizes L and $2L$ with increasing L . The value of ν obtained from the fourth-order cumulant at $L = 16$ coincides within the error-bars with the $L = 32$ result. The convergence of the ν computed from NN is worse. The $L = 16$

and $L = 32$ results are off by more than three times the error-bars. We also performed a two parameter fit to eq.(3.4). The estimates of the fits are given in Table VII. When we discard the data stemming from the $L = 4$ and 8 lattices, we get a $\frac{\chi^2}{dof}$ smaller than 1. If we take the uncertainty of the critical coupling into account we obtain the following values for the exponent ν :

Estimates of ν		
U_L	$U_{L/2}$	NN
0.6639(38)	0.6592(23)	0.6924(23)

One has to note that a small $\frac{\chi^2}{dof}$ does not mean that errors due to corrections to scaling are negligible. We have seen in the discussion of the cumulants that NN is much more affected by corrections to scaling than the fourth-order cumulant. Hence the result for ν obtained from NN should not be taken too seriously. As our final result, we take the value $\nu = 0.664(4)$ obtained from the fourth-order cumulant on the full lattice.

In order to estimate the ratio γ/ν of the critical exponents we studied the scaling behaviour of the magnetic susceptibility defined on the full lattice and on sub-blocks.

The dependence of the susceptibility on the lattice size at the critical point is given by eq.(2.9). We have estimated γ/ν from pairs of lattices with size L_1, L_2 . The ratio then is given by

$$\frac{\gamma}{\nu} = \frac{\ln(\chi(L_1, K_c)) - \ln(\chi(L_2, K_c))}{\ln(L_1) - \ln(L_2)}. \quad (3.7)$$

Table VIII shows the estimates of the ratio. The estimates for γ/ν obtained from the sub-blocks increase with increasing lattice size L , while those obtained from the full lattice decrease. We also performed a two-parameter fit following eq.(2.9). We could not extract reliable estimates for the ratio from the fits. However, the estimates of γ/ν from χ_L and $\chi_{L/2}$ obtained from the largest lattices coincide within the error-bars. Hence we take $\gamma/\nu = 1.973(9)$ obtained from the ratio of χ_L of the largest lattices as our final result, where statistical as well as systematic errors should be covered. Using the scaling relation $\eta = 2 - \frac{\gamma}{\nu}$, we obtain for the anomalous dimension $\eta = 0.027(9)$.

D. Symmetry of the order parameter

In a qualitative fashion we also looked at the symmetry of the order parameter \vec{M} . In figs. 3 a)–c) we have plotted the probability distribution of \vec{M} at $K = 2.0$ on lattices with $L = 8, 16$ and 32. Fig. 3 b) shows that the probability distribution for $L = 16$ is strongly peaked at six locations. Three of these peaks are considerably larger than the other ones.

This can be understood as follows. Configurations of minimal energy are reached when on one sub-lattice all spins take the same value while on the other sub-lattice the spins can

take any of the other two values [5]. The cluster algorithm easily manages to change the value of the spin on the ordered sub-lattice, while it takes many updates to switch the order from one sub-lattice to the other. For increasing L the peaks become more pronounced and the tunnelling times between the two metastable states increase.

In c) ($L = 32$) the simulation time (we have plotted 5000 measurements of the order parameter at $K = 2.0$) was not large enough to see a flip of the ordered state from one sub-lattice to the other, while for $L = 4$ the tunnelling time is much smaller than the simulation time.

Figs. 3 d)–e) show the probability distribution of the order parameter on lattices with $L = 8, 16$ and 32 at $K = 0.8157$ near the estimate of the critical coupling. In contrast to the situation at low temperature $K = 2.0$ we could not observe deviations from $U(1)$ invariance at the critical point on any of the considered lattices. Thus the Potts model seems to restore $U(1)$ symmetry at the critical point.

For short range interactions a universality class should be characterized by the dimensionality of the system and the symmetry of the order parameter at criticality [19]. Hence we conclude from the distribution of the order parameter at the critical point of the 3-state Potts model, that this model shares the universality class with the XY model.

E. Performance of the Algorithm

The efficiency of a stochastic algorithm is characterized by the integrated autocorrelation time

$$\tau_{int} = \frac{1}{2} \sum_{t=-\infty}^{\infty} \rho(t), \quad (3.8)$$

where the normalized autocorrelation function $\rho(t)$ of an observable A is given by

$$\rho(t) = \frac{\langle A_i \cdot A_{i+t} \rangle - \langle A \rangle^2}{\langle A^2 \rangle - \langle A \rangle^2}. \quad (3.9)$$

We calculated the integrated autocorrelation times τ_{int} with a self-consistent truncation window of width $6\tau_{int}$ for the energy density E and the magnetic susceptibility χ for lattices with $L = 4$ up to $L = 64$ at the coupling $K = 0.8157$. Our estimates for the critical dynamical exponents are $z_E = 0.18(3)$ and $z_\chi = 0.09(3)$ taking only statistical errors into account. Note that these exponents are consistent with those found in cluster simulations of the 3D XY model [20,17].

Finally let us briefly comment on the CPU time. 160 single cluster updates of the 64^3 lattice at the coupling $K = 0.8157$ plus one measurement of the observables took on average 20 sec CPU time on a IBM RISC 6000-550 workstation. For comparison, 160 single cluster updates of the 64^3 lattice at the coupling $K = 0.45417$ of the 3D XY model took on average 26 sec CPU time on the same machine [17]. All our MC simulations of the 3D AF Potts model together took about one month of CPU-time on an IBM RISC 6000-590 workstation where the simulations were done.

IV. DISCUSSION OF THE RESULTS

In this section we compare our results with those obtained in previous studies of the 3D AF 3-state Potts model. Furthermore we compare the AF 3-state Potts results with critical exponents and amplitudes obtained for 3D $O(N)$ -vector models. In Table X we display estimates for the critical properties of the 3D AF 3-state Potts model and the 3D XY model.

Our value for K_c agrees with the value obtained from the MC study by Wang et al. [7] within the error-bars. However, our error estimate is about 15 times more accurate. The Monte Carlo result for K_c given by Hoppe and Hirst [4] is consistent with our value within twice their error estimate, while our error estimate is about 84 times smaller than the error they quote. Yasumura et al. [21] obtained from the high temperature series expansion a result for K_c that is about 350 times our error-bar larger than our value. One has to note that they did not extract an estimate of the error.

The estimate for the ratio γ/ν that we obtain is consistent with the one given by Wang et al. [7]. Even taking into account systematic errors, we could reduce the uncertainty by about a factor of 3. Ueno et al. [6] calculated the ratio γ/ν via an interface approach. Their estimate is about 40 times their error-bar smaller than our value, while our error is about 2 times smaller than the one they quote. Hence we can rule out their result with high confidence.

The ratio γ/ν obtained from a MC study of the 3D XY model by the authors [17] is in excellent agreement with the one obtained in this work for the 3D Potts model. Our value for the ratio γ/ν is also consistent within the error-bars with the value obtained from resummed perturbation series of the 2-component ϕ^4 theory in 3D by Guillou and Zinn-Justin [9].

Our estimate of ν coincides within the error-bar with the value of the MC study of Wang et al. [7] while our error is about 6 times smaller than their error estimate. The value for ν given by Ueno et al. [6] is about 8 times their error-bar smaller than our value, while our error estimate is about 3 times smaller.

Our estimate for the exponent ν agrees within the error-bars with the one obtain for the 3D XY model in a MC study by the authors [17]. Moreover it is consistent within the quoted error-bars with the estimate obtained by resummed perturbation series of the 2-component ϕ^4 theory in 3D by Guillou and Zinn-Justin [9].

The most accurate value of ν is obtained in a ^4He experiment by Ahlers and Goldner [22]. Our estimate of ν is consistent with the experimental estimate of ν for ^4He within two times our error estimate. The experimental value is about 3 times more accurate than our result.

In order to judge the relevance of this nice agreement of the exponent ν of the 3D AF 3-state Potts model and the 3D 2-component ϕ^4 theory, one should note that Landau and Ferrenberg obtained [23] $\nu = 0.6289(8)$ in a Monte Carlo study of the 3D Ising model, which is consistent with the resummed perturbation theory result for the 1-component ϕ^4 theory $\nu = 0.6300(15)$ [9].

The value $\nu = 0.704(6)$ obtained in a Monte Carlo study of the 3D $O(3)$ model by Janke

and Holm [24], which can be compared with the 3-component ϕ^4 theory result $\nu = 0.705(3)$ [9] is also clearly inconsistent with the AF 3-state Potts value.

There exists no previous published result for the fourth-order cumulant of the order parameter \vec{M} . Hence we have to restrict our comparison to results for the 3D XY model and the 2-component ϕ^4 theory. Our estimate coincides with the one for the 3D XY model [17] within the error-bars. But the value obtained from the ϵ -expansion of the 2-component ϕ^4 theory of Brézin and Zinn-Justin [25] is off by 57 times our error estimate. Note that the relative error of the fourth-order cumulant obtained in this work is of order 0.1% taking into account the uncertainty of the critical coupling.

The results obtained in Monte Carlo studies of the 3D Ising model by Landau and Ferrenberg [23] $U_\infty \approx 0.47$, and one of the authors [26] $U_\infty = 0.464(2)$ are clearly off from our result $U_\infty = 0.5862(6)$ for the 3D AF 3-state Potts model. The fourth-order cumulant of the 3D $O(3)$ Heisenberg model, where the best value $U_\infty = 0.6217(8)$ stems from Monte Carlo simulation [24] is also far off from the 3D AF 3-state Potts result.

V. CONCLUSIONS

In the present work we have applied the single cluster algorithm [14] for the simulation of the 3D AF Potts model. The analysis of the critical dynamical behaviour shows that the algorithm is almost free of critical slowing down. Thus we were able to increase the statistics considerably by extensive use of modern RISC workstations.

The phenomenological RG approach allowed us to determine the critical amplitudes of the model with an accuracy of about 0.1%. From the fit of the crossings of the fourth-order cumulant we obtain for the critical coupling of the model $K_c = 0.81563(3)$, which reduces the error of an earlier MC study by a factor of about 15.

The excellent agreement of the universal critical amplitudes and exponents of the 3D AF Potts model with the ones of the 3D XY model strongly favours the supposition that the two models belong to the same universality class.

ACKNOWLEDGMENTS

We would like to thank S. Meyer for stimulating discussions on the subject, and A. Kavalov for a careful reading of the manuscript. The numerical simulations were performed on an IBM RISC 6000 cluster of the Regionales Hochschulrechenzentrum Kaiserslautern (RHRK). One of us (A.G.) expresses his gratitude for the hospitality he enjoyed during a visit to CERN.

REFERENCES

- [1] See, for example:
J.B. Kogut, Rev.Mod.Phys. **55**, 775 (1983).
- [2] See, for example:
J.M. Kosterlitz and D.J. Thouless, J.Phys. **C6**, 1181 (1973);
J.M. Kosterlitz, J.Phys. **C7**, 1046 (1974);
S.T. Chui and J.D. Weeks, Phys.Rev. **B14**, 4978 (1976);
J.V. José, L.P. Kadanoff, S. Kirkpatrick and D.R. Nelson, Phys.Rev. **B16**, 1217 (1977);
T. Ohta and K. Kawasaki, Prog.Theor.Phys. **60**, 365 (1978).
- [3] J.R. Banavar, G.S. Grest, and D. Jasnow, Phys.Rev.Lett. **45**, 1424 (1980);
J.R. Banavar, G.S. Grest, and D. Jasnow, Phys.Rev. **B25**, 4639 (1982).
- [4] B. Hoppe and L.L. Hirst, J. Phys. **A18**, 3375 (1985);
B. Hoppe and L.L. Hirst, Phys.Rev. **B34**, 6589 (1986).
- [5] I. Ono, Prog.Theor.Phys.Suppl. **87**, 102 (1986).
- [6] Y. Ueno, G. Sun and I. Ono, J.Phys.Soc.Jpn. **58**, 1162 (1989).
- [7] J.-S. Wang, R.H. Swendsen, and R. Kotecký, Phys.Rev.Lett. **63**, 109 (1989);
J.-S. Wang, R.H. Swendsen, and R. Kotecký, Phys.Rev. **B42**, 2465 (1990).
- [8] K.G. Wilson and M.E. Fisher, Phys. Rev. Lett. **28**, 240 (1972).
- [9] J.C. Le Guillou and J. Zinn-Justin, Phys. Rev. **B21**, 3976 (1980).
- [10] J.C. Le Guillou and J. Zinn-Justin, J. Phys. Lett. (Paris) **46**, L137 (1985).
- [11] V. Privman, P.C. Hohenberg, and A. Aharony, In *Phase Transitions and Critical Phenomena*, Vol 14, C. Domb and J.L. Lebowitz, eds. (Academic Press, London, 1991).
- [12] Preliminary results for the values of the cumulants at $K = 0.8157$ on lattices up to $L = 32$ by M. Hasenbusch and S. Meyer were reported by S. Meyer in a seminar talk at DESY in February 1990.
- [13] K. Binder, Phys.Rev.Lett. **47**, 693 (1981);
K. Binder, Z. Phys. **B43**, 119 (1981).
- [14] U. Wolff, Phys. Rev. Lett. **62**, 361 (1989);
U. Wolff, Nucl. Phys. **B322**, 759 (1989).
- [15] A.M. Ferrenberg and R.H. Swendsen, Phys. Rev. Lett. **61**, 2635 (1988).
- [16] R.G. Miller, Biometrika **61**, 1 (1974);

- B. Efron, *The Jackknife, the Bootstrap and other Resampling Plans* (SIAM, Philadelphia, PA, 1982).
- [17] A.P. Gottlob and M. Hasenbusch, *Physica* **A201**, 593 (1993).
 - [18] F.J. Wegner, *Phys. Rev.* **B5**, 4529 (1972).
 - [19] L.P. Kadanoff, In *Phase Transitions and Critical Phenomena* Vol. 5A, C. Domb and M.S. Green, eds. (Academic Press, London,1976).
 - [20] W. Janke, *Phys. Lett.* **A148**, 306 (1990).
 - [21] K. Yasumura and T. Oguchi, *J. Phys. Soc. Jpn.* **53**, 515 (1984).
 - [22] L.S. Goldner and G. Ahlers, *Phys. Rev.* **B45**, 13129 (1992).
 - [23] A.M. Ferrenberg and D.P. Landau, *Phys. Rev.* **B44**, 5081 (1991).
 - [24] C. Holm and W. Janke, *Phys.Lett* **A173**, 8 (1993).
 - [25] E. Brézin and J. Zinn-Justin, *Nucl. Phys.* **B257**, 867 (1985).
 - [26] M. Hasenbusch, *Physica* **A197**, 423 (1993).

FIGURES

FIG. 1. Reweighting plots from the simulations at $K_0 = 0.8157$. The dotted lines give the statistical error obtained by a Jackknife analysis. a) shows the cumulant defined on the full lattice, b) shows the reweighting of the cumulant defined on half of the lattice and c) shows the reweighting of the nearest neighbour product NN .

FIG. 2. Plot of the crossing couplings of the reweighted cumulants. Since the statistical error of the reweighted cumulants is small, one is able to see systematic convergence of the crossing couplings towards the critical coupling K_c .

FIG. 3. Plot of the probability distribution of the order parameter \vec{M} . The figures a) to c) show the distribution for $K = 2.0$ on lattices with $L = 8, 16$ and 32 . The figures from d) to f) show the probability distribution for $K = 0.8157$ near the final estimate of the critical coupling on lattices with $L = 8, 16$ and 32 .

TABLES

TABLE I. Results of the energy density E , the susceptibility defined on the full lattice (χ_L) and defined on the sub-blocks of size $L/2$ ($\chi_{L/2}$). The data is obtained from simulations at the fixed coupling $K_0 = 0.8157$ near the final estimate of the critical coupling. τ denotes the integrated autocorrelation time of the specified observable, given in units of the average number of clusters that is needed to cover the volume of the lattice. The statistics are given in terms of N measurements taken every N_0 update steps.

L	N	N_0	E	τ_E	χ_L	τ_χ	$\chi_{L/2}$
4	200k	10	0.1064(1)	0.55(1)	16.59(2)	0.54(1)	21.51(1)
8	200k	20	0.12383(4)	0.61(1)	69.54(7)	0.56(1)	80.53(6)
16	200k	40	0.13006(2)	0.64(1)	281.01(33)	0.57(1)	314.34(28)
32	200k	80	0.132267(7)	0.71(1)	1120.8(1.3)	0.60(1)	1239.7(1.1)
64	170k	160	0.133062(3)	0.82(2)	4447.8(5.9)	0.64(2)	4890.2(4.9)

TABLE II. Estimates of the couplings at the crossings of the the reweighted cumulants. $L_1 - L_2$ denotes the lattices used to determine the crossing.

Crossing couplings K_{cross}			
$L_1 - L_2$	$K_{cross}(U_L)$	$K_{cross}(U_{L/2})$	$K_{cross}(NN)$
4-8	0.82941(46)	0.84403(33)	0.76580(50)
8-16	0.81844(15)	0.81916(10)	0.80837(13)
16-32	0.816202(53)	0.816345(43)	0.814728(41)
32-64	0.815737(20)	0.815795(15)	0.815529(14)

TABLE III. Estimates of the critical couplings from the fit following eq.(3.2) with $\nu = 0.669$ and $\omega = 0.78$ being fixed. # gives the number of discarded data points with small L .

K_c from U_L			
#	K_c	C_{U_L}	$\frac{\chi^2}{dof}$
0	0.815619(20)	0.403(12)	0.006
1	0.815619(22)	0.404(21)	0.011
K_c from $U_{L/2}$			
#	K_c	$C_{U_{L/2}}$	$\frac{\chi^2}{dof}$
0	0.815530(15)	0.729(8)	185.0
1	0.815647(16)	0.499(14)	0.198
K_c from NN			
#	K_c	C_{NN}	$\frac{\chi^2}{dof}$
0	0.815987(14)	-1.244(11)	263
1	0.815854(15)	-0.964(17)	76.9

TABLE IV. Estimates of the cumulants at our best estimate of the critical coupling $K_c = 0.81563(3)$.

Estimates of U_L			
L	$K_c - \Delta K_c$	K_c	$K_c + \Delta K_c$
4	0.60975(21)	0.60976(21)	0.60977(21)
8	0.59985(25)	0.59989(25)	0.59993(24)
16	0.59367(25)	0.59378(25)	0.59388(25)
32	0.58981(26)	0.59012(26)	0.59042(26)
64	0.58724(28)	0.58812(28)	0.58899(27)
Estimates of $U_{L/2}$			
L	$K_c - \Delta K_c$	K_c	$K_c + \Delta K_c$
4	0.58449(11)	0.58450(11)	0.58451(11)
8	0.56479(15)	0.56482(15)	0.56486(15)
16	0.55700(18)	0.55711(18)	0.55721(18)
32	0.55223(20)	0.55253(20)	0.55283(20)
64	0.54863(22)	0.54949(21)	0.55035(21)
Estimates of NN			
L	$K_c - \Delta K_c$	K_c	$K_c + \Delta K_c$
4	0.67621(36)	0.67624(36)	0.67627(36)
8	0.76378(32)	0.76385(32)	0.76392(32)
16	0.79269(29)	0.79286(29)	0.79303(29)
32	0.80158(28)	0.80205(28)	0.80251(28)
64	0.80351(30)	0.80479(30)	0.80606(30)

TABLE V. Estimates of the cumulants from the fit following eq.(3.3). # gives the number of discarded data-points with small L .

Estimates of U_L									
$K_c - \Delta K_c$			K_c			$K_c + \Delta K_c$			
#	U_L	C_{U_L}	$\frac{\chi^2}{dof}$	U_L	C_{U_L}	$\frac{\chi^2}{dof}$	U_L	C_{U_L}	$\frac{\chi^2}{dof}$
0	0.58486(20)	0.1264(16)	2.64	0.58541(20)	0.1231(16)	0.53	0.58595(20)	0.1198(16)	0.87
1	0.58511(22)	0.1271(33)	7.31	0.58560(22)	0.1227(33)	2.43	0.58608(21)	0.1184(32)	1.14
2	0.58567(27)	0.1165(66)	10.07	0.58605(27)	0.1128(66)	3.01	0.58643(27)	0.1089(66)	0.53
Estimates of $U_{L/2}$									
$K_c - \Delta K_c$			K_c			$K_c + \Delta K_c$			
#	$U_{L/2}$	$C_{U_{L/2}}$	$\frac{\chi^2}{dof}$	$U_{L/2}$	$C_{U_{L/2}}$	$\frac{\chi^2}{dof}$	$U_{L/2}$	$C_{U_{L/2}}$	$\frac{\chi^2}{dof}$
0	0.54308(14)	0.2218(11)	87.50	0.54360(14)	0.2184(11)	104	0.54410(14)	0.2152(11)	125
1	0.54580(16)	0.1764(24)	10.84	0.54625(16)	0.1721(24)	2.82	0.54673(16)	0.1676(24)	0.09
2	0.54608(20)	0.1729(53)	14.34	0.54643(20)	0.1695(53)	3.83	0.54682(20)	0.1650(53)	0.01
Estimates of NN									
$K_c - \Delta K_c$			K_c			$K_c + \Delta K_c$			
#	NN	C_{NN}	$\frac{\chi^2}{dof}$	NN	C_{NN}	$\frac{\chi^2}{dof}$	NN	C_{NN}	$\frac{\chi^2}{dof}$
0	0.83152(23)	-0.5034(15)	2048	0.83240(23)	-0.5068(15)	1949	0.83327(23)	-0.5102(15)	1855
1	0.81677(25)	-0.3083(28)	187	0.81751(25)	-0.3127(28)	170	0.81825(25)	-0.3171(28)	158
2	0.81176(30)	-0.2010(54)	19.19	0.81233(30)	-0.2048(54)	8.06	0.81290(30)	-0.2085(54)	5.08

TABLE VI. Estimates of the critical exponent ν obtained from the slope of the cumulants at $K_c = 0.81563(3)$ using eq.(3.6).

Estimates of ν from the data of U_L			
$L_1 - L_2$	$K_c - \Delta K_c$	K_c	$K_c + \Delta K_c$
4-8	0.6330(58)	0.6332(58)	0.6334(58)
8-16	0.6543(67)	0.6548(67)	0.6552(67)
16-32	0.6617(83)	0.6628(83)	0.6639(83)
32-64	0.6584(99)	0.6615(99)	0.6646(99)
Estimates of ν from the data of $U_{L/2}$			
$L_1 - L_2$	$K_c - \Delta K_c$	K_c	$K_c + \Delta K_c$
4-8	0.5628(27)	0.5628(27)	0.5629(27)
8-16	0.6391(40)	0.6393(40)	0.6395(40)
16-32	0.6540(52)	0.6546(52)	0.6552(52)
32-64	0.6601(65)	0.6617(64)	0.6634(64)
Estimates of ν from the data of NN			
$L_1 - L_2$	$K_c - \Delta K_c$	K_c	$K_c + \Delta K_c$
4-8	0.8095(57)	0.8097(57)	0.8099(57)
8-16	0.7451(49)	0.7456(49)	0.7460(49)
16-32	0.6963(44)	0.6974(44)	0.6984(44)
32-64	0.6819(52)	0.6847(52)	0.6877(52)

TABLE VII. Estimates of the critical exponent ν obtained from the fit of cumulants following eq.(3.4) at $K_c = 0.81563(3)$. # gives the number of discarded data-points with small L .

Estimates of ν from the data of U_L									
$K_c - \Delta K_c$			K_c			$K_c + \Delta K_c$			
#	ν	C_ν	$\frac{\chi^2}{dof}$	ν	C_ν	$\frac{\chi^2}{dof}$	ν	C_ν	$\frac{\chi^2}{dof}$
0	0.6513(18)	0.0505(5)	4.49	0.6522(18)	0.0507(5)	5.09	0.6532(17)	0.0509(5)	5.79
1	0.6598(22)	0.0536(8)	0.58	0.6605(22)	0.0538(8)	0.38	0.6613(22)	0.0540(8)	0.34
2	0.6635(34)	0.0552(15)	0.39	0.6638(34)	0.0553(15)	0.10	0.6642(34)	0.0553(15)	0.01
Estimates of ν from the data of $U_{L/2}$									
$K_c - \Delta K_c$			K_c			$K_c + \Delta K_c$			
#	ν	C_ν	$\frac{\chi^2}{dof}$	ν	C_ν	$\frac{\chi^2}{dof}$	ν	C_ν	$\frac{\chi^2}{dof}$
0	0.6216(9)	0.0386(2)	186	0.6222(9)	0.0387(2)	190	0.6229(9)	0.0389(2)	195
1	0.6518(14)	0.0490(5)	4.90	0.6522(14)	0.0491(5)	4.81	0.6526(14)	0.0492(5)	4.86
2	0.6590(21)	0.0521(9)	0.61	0.6592(21)	0.0521(9)	0.36	0.6594(21)	0.0522(9)	0.25
Estimates of ν from the data of NN									
$K_c - \Delta K_c$			K_c			$K_c + \Delta K_c$			
#	ν	C_ν	$\frac{\chi^2}{dof}$	ν	C_ν	$\frac{\chi^2}{dof}$	ν	C_ν	$\frac{\chi^2}{dof}$
0	0.7347(13)	0.1377(9)	166	0.7355(13)	0.1380(9)	161	0.7363(13)	0.1384(9)	156
1	0.7066(14)	0.1160(11)	31.39	0.7073(14)	0.1163(11)	30.57	0.7080(14)	0.1166(11)	30.07
2	0.6920(19)	0.1038(15)	1.48	0.6924(19)	0.1039(15)	0.82	0.6928(19)	0.1040(15)	0.69

TABLE VIII. Estimates of the ratio γ/ν obtained from the susceptibility at $K_c = 0.81563(3)$ using equation (3.7).

Estimates of γ/ν from the data of χ_L			
$L_1 - L_2$	$K_c - \Delta K_c$	K_c	$K_c + \Delta K_c$
4-8	2.0663(20)	2.0667(20)	2.0669(20)
8-16	2.0119(23)	2.0128(23)	2.0136(23)
16-32	1.9878(24)	1.9902(24)	1.9927(24)
32-64	1.9660(25)	1.9728(25)	1.9796(25)
Estimates of γ/ν from the data of $\chi_{L/2}$			
$L_1 - L_2$	$K_c - \Delta K_c$	K_c	$K_c + \Delta K_c$
4-8	1.9035(14)	1.9039(14)	1.9041(14)
8-16	1.9630(16)	1.9635(16)	1.9642(16)
16-32	1.9735(18)	1.9754(18)	1.9773(18)
32-64	1.9625(19)	1.9677(19)	1.9729(19)

TABLE IX. Estimates of the ratio γ/ν obtained from the fit of the susceptibility following eq.(2.9) at $K_c = 0.81563(3)$. # gives the number of discarded data-points with small L .

Estimates of γ/ν from the data of χ_L									
	$K_c - \Delta K_c$			K_c			$K_c + \Delta K_c$		
#	γ/ν	$C_{\gamma/\nu}$	$\frac{\chi^2}{dof}$	γ/ν	$C_{\gamma/\nu}$	$\frac{\chi^2}{dof}$	γ/ν	$C_{\gamma/\nu}$	$\frac{\chi^2}{dof}$
0	2.0107(5)	1.0394(14)	500	2.0128(5)	1.0356(14)	448	2.0149(5)	1.0320(14)	399
1	1.9910(6)	1.1128(24)	64.16	1.9927(6)	1.1091(24)	46.56	1.9943(6)	1.1054(24)	39.61
2	1.9835(10)	1.1468(42)	29.64	1.9844(10)	1.1452(42)	9.48	1.9854(10)	1.1436(42)	3.74
Estimates for γ/ν from the data of $\chi_{L/2}$									
	$K_c - \Delta K_c$			K_c			$K_c + \Delta K_c$		
#	γ/ν	$C_{\gamma/\nu}$	$\frac{\chi^2}{dof}$	γ/ν	$C_{\gamma/\nu}$	$\frac{\chi^2}{dof}$	γ/ν	$C_{\gamma/\nu}$	$\frac{\chi^2}{dof}$
0	1.9518(4)	0.2022(2)	524	1.9535(4)	0.2016(2)	568	1.9552(4)	0.2010(2)	620
1	1.9693(5)	0.1911(3)	28.52	1.9706(5)	0.1907(3)	12.96	1.9719(5)	0.1902(3)	8.53
2	1.9733(7)	0.1885(5)	30.10	1.9741(7)	0.1882(5)	7.76	1.9749(7)	0.1880(5)	0.74

TABLE X. Comparison of critical properties of the 3D AF Potts model and the 3D XY model determined by various methods.

Method	Ref.	K_c	γ/ν	ν	U_L
3D AF Potts model					
Phenomenological RG	this work	0.81563(3)	1.973(9)	0.6639(38)	0.5862(6)
Phenomenological RG	[7]	0.8157(5)	1.99(3)	0.66(3)	–
Interface approach	[6]	0.810	1.10(2)	0.58(1)	–
MC	[5]	0.80	–	–	–
MC	[4]	0.781(25)	–	–	–
High temperature series	[21]	0.826	–	–	–
3D XY model					
Phenomenological RG	[17]	0.45419(2)	1.976(6)	0.662(7)	0.5875(28)
High temperature MC	[17]	0.454170(7)	–	–	–
Resummed perturbation series	[9]	–	1.967(4)	0.669(2)	–
ϵ -expansion	[25]	–	–	–	0.552
Experiment ^4He	[22]	–	–	0.6705(6)	–

FIG. 1 a)

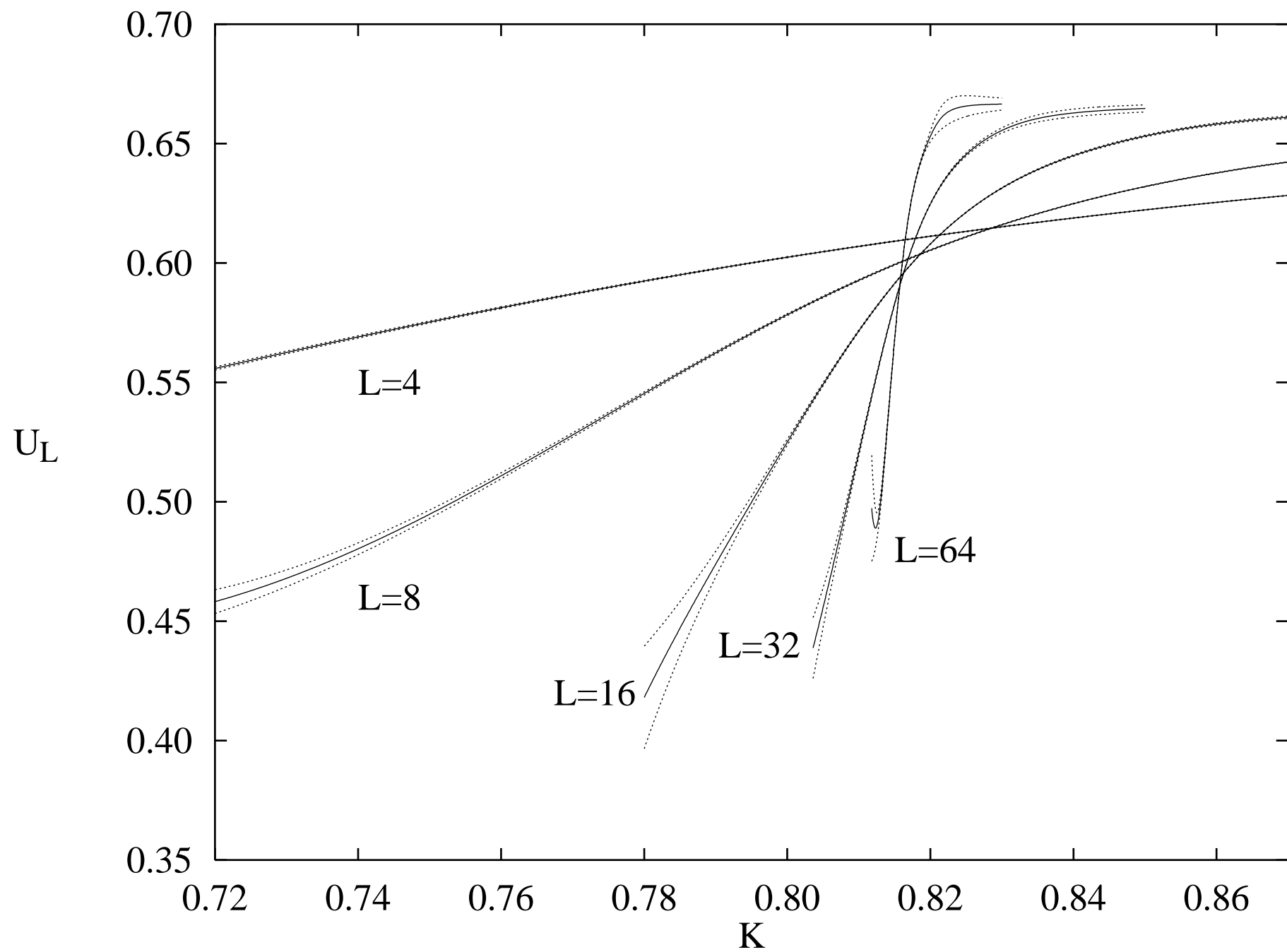


FIG. 1 b)

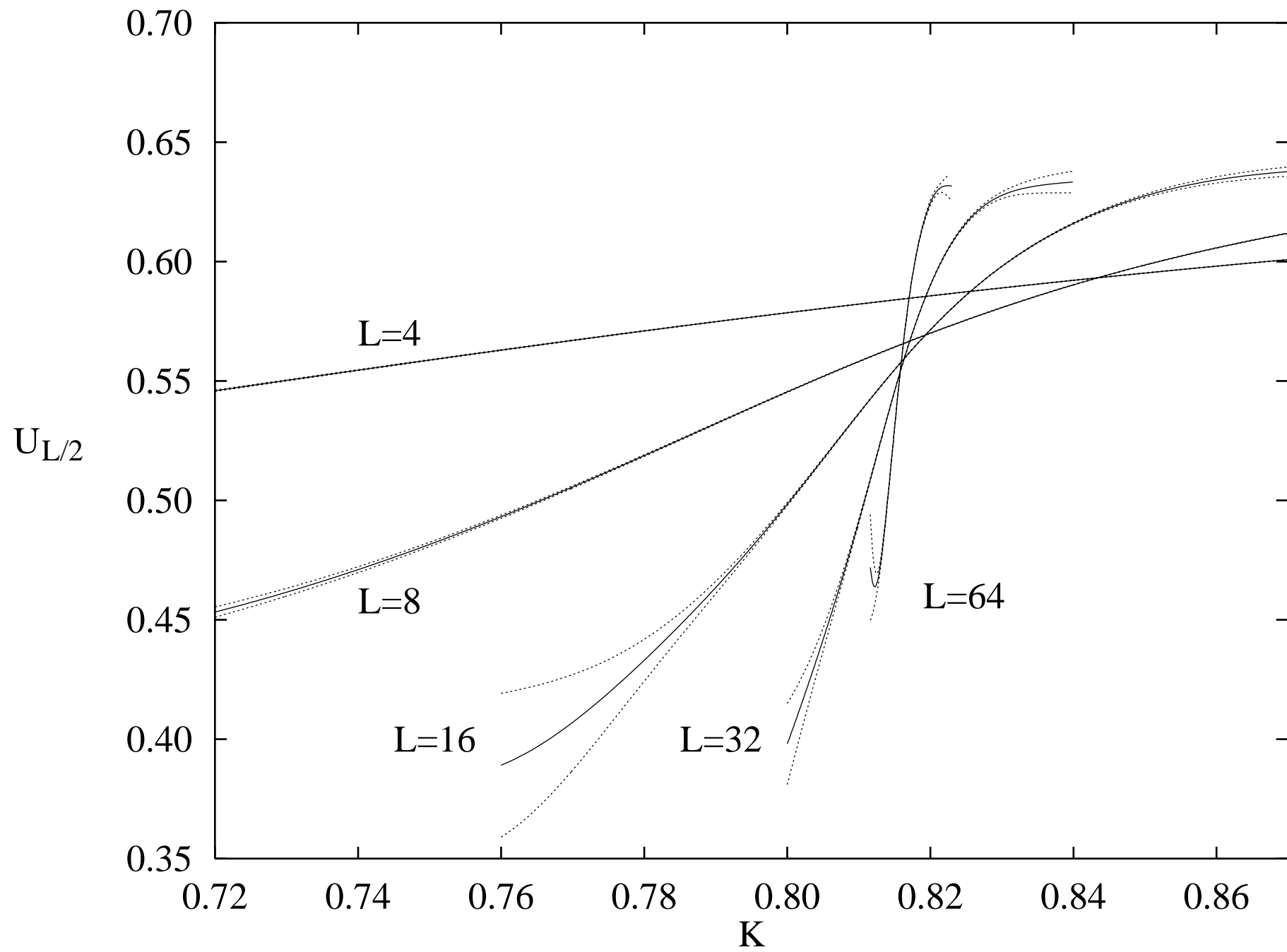


FIG. 1 c)

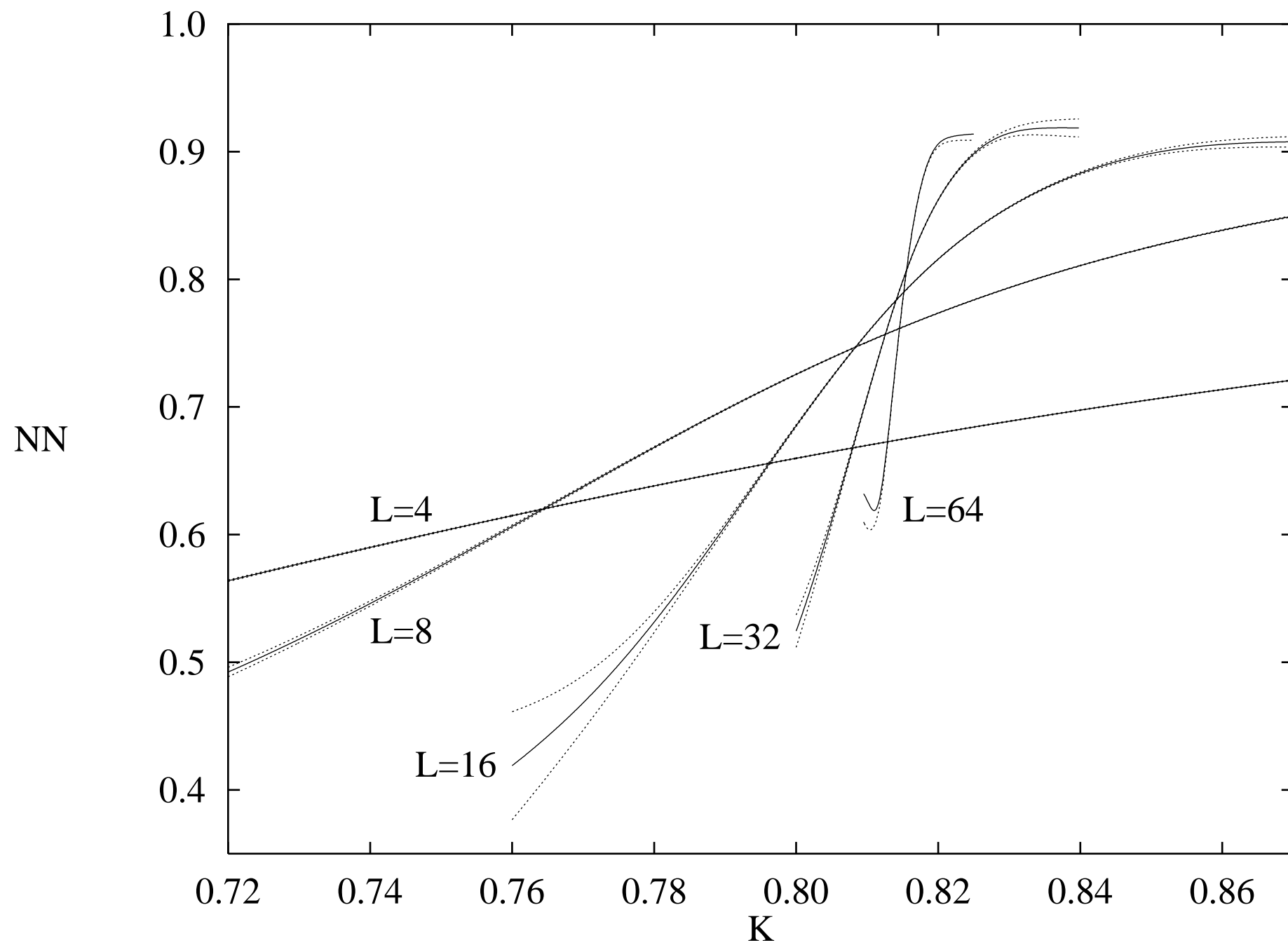


FIG. 2

